European Radiology (2018) 28:5001–5009
https://doi.org/10.1007/s00330-018-5513-0

MAGNETIC RESONANCE

Proton density fat fraction (PDFF) MR imaging for differentiation of acute benign and neoplastic compression fractures of the spine

Frederic Carsten Schmeel[1] · Julian Alexander Luetkens[1] · Simon Jonas Enkirch[1] · Andreas Feißt[1] · Christoph Hans-Jürgen Endler[1] · Leonard Christopher Schmeel[1] · Peter Johannes Wagenhäuser[1] · Frank Träber[1] · Hans Heinz Schild[1] · Guido Matthias Kukuk[1]

Received: 26 February 2018 / Revised: 18 April 2018 / Accepted: 26 April 2018 / Published online: 1 June 2018

Abstract

Objectives To evaluate the diagnostic performance of proton density fat fraction (PDFF) magnetic resonance imaging (MRI) to differentiate between acute benign and neoplastic vertebral compression fractures (VCFs).

Methods Fifty-seven consecutive patients with 46 acute benign and 41 malignant VCFs were prospectively enrolled in this institutional review board approved study and underwent routine clinical MRI with an additional six-echo modified Dixon sequence of the spine at a clinical 3.0-T scanner. All fractures were categorised as benign or malignant according to either direct bone biopsy or 6-month follow-up MRI. Intravertebral PDFF and $PDFF_{ratio}$ (fracture PDFF/normal vertebrae PDFF) for benign and malignant VCFs were calculated using region-of-interest analysis and compared between both groups. Additional receiver operating characteristic and binary logistic regression analyses were performed.

Results Both PDFF and $PDFF_{ratio}$ of malignant VCFs were significantly lower compared to acute benign VCFs [PDFF, 3.48 ± 3.30% vs 23.99 ± 11.86% ($p < 0.001$); $PDFF_{ratio}$, 0.09 ± 0.09 vs 0.49 ± 0.24 ($p < 0.001$)]. The areas under the curve were 0.98 for PDFF and 0.97 for $PDFF_{ratio}$, yielding an accuracy of 96% and 95% for differentiating between acute benign and malignant VCFs. PDFF remained as the only imaging-based variable to independently differentiate between acute benign and malignant VCFs on multivariate analysis (odds ratio, 0.454; $p = 0.005$).

Conclusions Quantitative assessment of PDFF derived from modified Dixon water-fat MRI has high diagnostic accuracy for the differentiation of acute benign and malignant vertebral compression fractures.

Key Points

- *Chemical-shift-encoding based water-fat MRI can reliably assess vertebral bone marrow PDFF*
- *PDFF is significantly higher in acute benign than in malignant VCFs*
- *PDFF provides high accuracy for differentiating acute benign from malignant VCFs*

Keywords Magnetic resonance imaging · Chemical shift imaging · Spinal fractures · Compression fracture

Abbreviations

6E-mDixon	Six-echo modified Dixon
95%CI	95 % confidence interval
mDixon	Modified Dixon
NPV	Negative predictive value
PDFF	Proton density fat fraction
PET/CT	Positron emission tomography/computed tomography
PPV	Positive predictive value
ROC	Receiver operating characteristic
ROI	Region of interest
SE	Spin echo
SENSE	Sensitivity encoding
SPAIR	Spectral attenuated inversion recovery
TE	Echo time
TR	Repetition time
VCF	Vertebral compression fracture

✉ Frederic Carsten Schmeel
Carsten.Schmeel@ukb.uni–bonn.de

[1] Department of Radiology and Radiation Oncology, University Hospital Bonn, Rheinische-Friedrich-Wilhelms-Universität Bonn, Sigmund-Freud-Straße 25, 53127 Bonn, Germany

Introduction

The differentiation between acute osteoporotic and malignant vertebral compression fractures (VCFs) is a common clinical problem with considerable management and prognostic implications. Since VCFs associated with both osteoporosis and malignancy usually occur in elderly people, mostly without a history of an adequate trauma, the clinical differentiation between these two fracture types can be challenging [1]. Current evidence suggests that the incidence of unsuspected malignancy in bone biopsies obtained during vertebroplasty is approximately 5% [2]. Conventional magnetic resonance imaging (MRI) provides important information on signal abnormalities of bone marrow and adjacent soft tissue which can help to diagnose the underlying pathology [3]. However, despite numerous morphological criteria that may aid differentiating osteoporotic from malignant VCFs, it lacks specificity, especially in the acute setting [4]. This is because reactive inflammation and bone marrow oedema of acute osteoporotic fractures can mimic the signal alterations observed in cases with underlying malignancy, many of whom may lack a paravertebral mass [5]. Therefore, invasive bone biopsies are often necessary to establish a definitive diagnosis.

Osteoporotic VCFs usually contain fatty bone marrow pervaded with oedema, whereas malignant processes tend to completely replace the fatty bone marrow matrix [6, 7]. Hence, chemical-shift-encoded in-phase/opposed-phase MRI, which can demonstrate the presence of intracytoplasmic fat, has been used in musculoskeletal oncology to aid in the characterisation of benign from malignant VCFs [8–10]. Quantitative chemical-shift-encoding based water-fat MRI using spatially resolved proton density fat fraction (PDFF) maps is an emerging method to assess the vertebral bone marrow fat content [11, 12]. PDFF measurements have been validated against the chemically determined fat content in ex vivo water-fat trabecular bone phantoms and single-voxel MR spectroscopy based in vivo fat fraction estimations of spine marrow [13, 14]. Moreover, PDFF has been proposed for diagnosis and response assessment in patients undergoing anti-cancer treatment [15]. However, published knowledge on the usefulness of PDFF for differentiation of acute benign and malignant VCFs is currently unavailable.

Therefore, the purpose of this prospective study was to determine the diagnostic value of a six-echo modified Dixon (6E-mDixon) derived PDFF for the differentiation of acute benign and neoplastic VCFs.

Patient selection

This prospective study was granted institutional review board approval (approval no. 177/15, University of Bonn) and written informed consent from all study participants had been obtained prior evaluation. Between February 2015 and December 2017, 119 consecutive patients with a clinically suspected acute VCF or known primary malignancy and suspected VCF underwent routine clinical MRI of the spine with an additional 6E-mDixon sequence at 3.0-T. Fifty-seven of these patients (28 men, 29 women; mean age, 66.9 ± 15.7 years; range, 18-95 years) were prospectively enrolled because they met the following inclusion criteria: adult age, presence of an acute VCF and an acute (≤1 month) onset of back pain at the spinal level of the suspected VCF. To establish a diagnostic reference standard, further inclusion criteria were either histopathological confirmation of acute VCFs when clinically indicated, or, in cases in which histopathology could not be obtained, follow-up MRI after 6 months in combination with at least one of the following additional imaging studies: (1) computed tomography (CT) and/or (2) ^{18}F-fluorodeoxyglucose positron emission tomography/computed tomography (FDG-PET/CT) of the spine segment under investigation. Exclusion criteria for study participation were contraindications to MRI and metallic implants on the spinal level. Demographic and clinical characteristics of the study cohort are detailed in Table 1.

MR imaging

All imaging was performed on a clinical 3.0-T whole-body MR imager (Ingenia 3.0-T; Philips Healthcare, Eindhoven, The Netherlands). Routine clinical MRI of the spine included at least a sagittal T1-weighted spin-echo (450-750/6-12 ms [repetition time (TR)/echo time (TE)] and T2-weighted turbo spin-echo sequence [3,000-5,000/80-120 ms (TR/TE)] as well as a sagittal T2 spectral-attenuated-inversion-recovery (SPAIR)-weighted turbo spin-echo sequence [3,000-5,000/80-120 ms (TR/TE)]. Field of view, matrix size, slice thickness and interslice gap were adjusted to the specific site under study. Choice of receiver coils was dependent on the specific anatomic site using the posterior and/or total spine coil.

To determine the percentage PDFF, i.e. fat/(water + fat), a six-echo 3D gradient-echo modified Dixon sequence (mDixon Quant; Philips Healthcare) was acquired with equidistant echo spacing of 1.15 ms (first TE = 1.15 ms). The TR was fixed to the shortest possible TR in 6E-mDixon (8 ms). A very low spin flip angle of 3° was applied to avoid T1 saturation. With 80 reconstructed sagittal slices (overcontiguous with 2 mm offset, interpolated from 4 mm through-plane resolution), the vertebral coverage was 16 cm and the in-plane resolution of 2.5 mm was interpolated to 1.5 mm. Parallel imaging was used with a SENSE factor of 2 in the anterior-posterior direction and a factor of 1.5 in the slice encoding direction. Total scan time was 37 s acquired during two breath-holds. Parametric PDFF maps were automatically generated on the imager software from the 6E-mDixon examination.

Table 1 Demographic and clinical characteristics of the study cohort and acute benign and neoplastic vertebral compression fractures

Variable		Benign		Neoplastic		*p*
		n	%	*n*	%	
All patients		32	56	25	44	n.a.
Gender	Male	13	23	15	26	0.150
	Female	19	33	10	18	
Age in years (range)		67.56	(18-95)	65.96	(35-86)	0.699
Previous chemotherapy		9	16	20	35	<0.001*
Previous radiotherapy		6	11	10	16	0.079
All vertebral compression fractures		46	53	41	47	n.a.
No. of vertebral fractures per patient	1	19	35	14	25	0.505
	2-3	12	22	9	16	
	4-5	0	0	1	2	
Location of vertebral fractures	Cervical	3	3	1	1	0.878
	Thoracic	18	21	19	22	
	Lumbar	25	29	19	22	
	Sacral	0	0	2	2	
Age of vertebral fractures	Hyperacute (≤7 days old)	28	32	20	23	0.260
	Acute (≤30 days old)	18	21	21	24	
Thereof pathologically confirmed		21	24	24	28	0.459

* p <0.05 (statistically significant)

n.a. not applicable

Definition and diagnosis of acute vertebral compression fractures

Acute VCFs were defined as areas of bone marrow oedema within a deformed vertebral body [16]. Deformation was defined as a minimum 15% height loss in the anterior, middle or posterior dimension of a vertebral body (or any combination thereof) as assessed on T1-weighted and T2-SPAIR-weighted images [17].

The standard of reference was direct bone biopsy and histopathological confirmation in 30/57 patients (53%) having a total of 45/87 VCFs (52%). In the remaining 42 acute VCFs without available biopsy, the diagnosis was established on the basis of characteristic imaging appearance [18] on 6-month MR imaging follow-up showing either:

1. Complete resolution of bone marrow oedema on T1- and T2-SPAIR-weighted images and reconstitution of normal imaging appearance

   or

2. Progression of malignant lesions and persistence of bone marrow oedema.

Imaging criterion standards were determined by consensus reading of two experienced investigators under consideration of all acquired images including follow-up. VCFs were classified as either benign or malignant according to the diagnostic reference standard and subsequently divided into two groups.

Image analysis

In each patient, up to five VCFs were defined based on morphological MRI findings. Morphological MRI sequences and PDFF maps were cross-linked to ensure correct lesion detection and delineation. Two investigators placed free-hand regions of interest (ROIs) within the selected VCFs at a single slice with the largest possible lesion diameter. Each ROI was adapted to the hypointense signal on T1-weighted sagittal images and afterwards copied onto the corresponding PDFF map. Afterwards, the mean percentage PDFF value inside the ROI and the corresponding ROI size were recorded for each VCF. The mean PDFF values obtained by both investigators were averaged for each predefined VCF. In addition, mean percentage PDFF of unaffected vertebrae was determined using a circular ROI, as large as possible, on midline sagittal images. The ratio between the PDFF of VCFs and

normal vertebrae (i.e. fracture PDFF/normal vertebrae PDFF) was calculated and referred to as $PDFF_{ratio}$.

Statistical analysis

Statistical analyses were performed using SPSS v. 25 statistical software (IBM). Mean ± standard deviation was calculated for all applicable data, unless otherwise specified. Statistical significance level was defined as $p \leq 0.05$. Statistical power analyses revealed that 36 observations per group would provide sufficient power ($\beta = 0.9$) to show a significant difference between the two groups, assuming that the majority of malignant fractures would show lowered PDFF values (probability, 1:0.80) [19]. Inter-observer agreement regarding PDFF measures provided by both observers was assessed using Lin's concordance correlation coefficient (RC) and intra-class correlation coefficient (ICC). Mann–Whitney *U* test was used for inter-class comparisons of independent clinical and imaging data, and Wilcoxon signed-rank test was used for pairwise inter-class comparisons. Variables showing significant differences on univariate analysis at $p \leq 0.2$ were further analysed using binary logistic regression analysis in a forward conditional model to determine the relative contribution of imaging and clinical parameters for differentiation of acute benign and malignant VCFs. Receiver operating characteristic (ROC) curves were plotted to determine the optimal PDFF cut-off value in order to differentiate benign from malignant VCFs. Sensitivity, specificity, positive predictive value (PPV), negative predictive value (NPV) and accuracy were calculated using this threshold.

Results

Fifty-seven patients with a total of 87 VCFs were included in the analysis. The median and mean time interval between symptom onset referable to acute VCFs and 6E-mDixon spine MRI was 7 and 9 ± 7.9 days, respectively, ranging from 1-30 days.

Group 1 consisted of 32 patients (13 men, 19 women; mean age, 67.6 ± 16.8 years; range, 18-95 years) with 46 osteoporotic and/or benign VCFs. Diagnosis was established by direct bone biopsy and histopathological confirmation in 13/32 patients with 21 fractures. In 19/32 patients with 25 fractures, diagnosis was based on 6-month follow-up MRI showing full resolution of bone marrow oedema on T1- and T2-SPAIR-weighted images. In addition, no evidence of radiographic progression of vertebral destruction or significant FDG-uptake could be detected in these patients on additionally performed CT ($n = 19$) and/or FDG-PET/CT ($n = 2$) studies 1-7 months after the initial MRI.

Group 2 consisted of 25 patients (15 men, 10 women; mean age 66.0 ± 14.9; range, 35-86 years) with 41 neoplastic VCFs due to vertebral metastasis ($n = 30$) or haematological neoplasms ($n = 11$). Direct bone biopsy and histopathological confirmation was available in 17/25 patients with 24 fractures. The remaining eight patients with 17 fractures had multi-organ metastasis and pathological correlation was obtained from the malignant primary tumour or other metastatic sites. In these 8/25 patients, diagnosis of a neoplastic VCF was confirmed on the basis of typical imaging characteristics at 6-month follow-up MRI showing persisting oedema on T1- and T2-SPAIR-weighted images ($n = 17$), detection and/or size progression of an extraosseous soft-tissue mass ($n = 11$), progredient convex bulging of the posterior vertebral border ($n = 12$) and presence of other spinal metastases ($n = 17$). Additional CT ($n = 8$) and FDG-PET/CT ($n = 5$) studies were performed 1-3 months after the initial MRI showing destructive osseous processes and/or definitely increased FDG-uptake values within the affected vertebral bodies. Primary tumours in group 2 were prostate cancer ($n = 11$), lung cancer ($n = 7$), multiple myeloma ($n = 7$), breast cancer ($n = 5$), chronic lymphocytic leukaemia ($n = 3$), colorectal cancer ($n = 2$), head and neck cancer ($n = 2$), cholangiocarcinoma ($n = 1$), diffuse large B-cell lymphoma ($n = 1$), hepatocellular carcinoma ($n = 1$) and renal cancer ($n = 1$).

PDFF readout was performed in all acute benign and malignant VCFs with an ROI size of 212.87 ± 140.89 mm^2 (range, 60-857 mm^2). The RC was 0.993 (95% CI, 0.989-0.996), and ICC was 0.993 (95% CI, 0.990-0.996) as measure for the inter-observer agreement, suggesting an excellent agreement between the two readers for PDFF measurements.

The PDFF was significantly higher in benign VCFs than in cases with underlying malignancy (Table 2): mean PDFF for benign VCFs (Fig. 1) was 23.99 ± 11.86% and mean PDFF for neoplastic VCFs (Fig. 2) was 3.48 ± 3.30% ($p < 0.001$). Mean $PDFF_{ratio}$ for benign VCFs was 0.49 ± 0.24 and mean $PDFF_{ratio}$ for malignant VCFs was 0.09 ± 0.09 and also significantly different between the two groups ($p < 0.001$). Mean PDFF for normal vertebral bodies was 45.23 ± 14.47% and differed significantly from mean PDFF values for both benign ($p = 0.001$) and malignant VCFs ($p < 0.001$). Subclass PDFF values of benign and malignant VCFs are graphically illustrated in Fig. 3.

When further subdividing VCFs according to fracture age into hyperacute (≤7 days old) and acute (≤30 days old) stage, mean PDFF for hyperacute benign, acute benign, hyperacute malignant and acute malignant VCFs was 23.85 ± 12.95%, 24.21 ± 10.29%, 3.53 ± 3.89% and 3.43 ± 7.72%, respectively. There was no statistically significant difference in PDFF between the hyperacute and acute stage of both benign ($p = 0.70$) and malignant ($p = 0.83$) VCFs. Mean $PDFF_{ratio}$ was 0.48 ± 0.25 for hyperacute benign, 0.52 ± 0.23 for acute benign, 0.1 ± 0.13 for hyperacute malignant and 0.09 ± 0.06 for acute malignant

Table 2 Group differences between benign and neoplastic acute vertebral compression fractures

Variable		Benign		Neoplastic		*p*
		n	± SD	*n*	± SD	
Fracture PDFF	%	23.99	11.86	3.48	3.30	<0.001*
Normal vertebral body PDFF	%	50.47	11.97	38.74	14.99	<0.001*
$PDFF_{ratio}$		0.49	0.24	0.09	0.09	<0.001*
ROI size	mm^2	240	158	182	112	0.064

* $p < 0.05$ (statistically significant)

PDFF proton density fat fraction, *ROI* region of interest, *SD* standard deviation

VCFs, without a statistically significant difference in $PDFF_{ratio}$ between both the hyperacute and acute stage of benign ($p = 0.53$) and malignant ($p = 0.48$) VCFs.

ROC analysis revealed that using a PDFF cut-off value of ≤9% for malignancy was optimal to differentiate benign from malignant VCFs (Fig. 4): 45 of 46 benign and 39 of 41 malignant VCFs were correctly classified; one osteoporotic fracture had a PDFF below 9 %, while two VCFs in patients with multiple myeloma had a PDFF above the cut-off. This yielded a sensitivity of 98%, a specificity of 95% with a corresponding AUC of 98% (95% CI, 96-100%; $p < 0.001$), a PPV of 94%, an NPV of 98% and an accuracy of 96% in the differentiation of benign from malignant VCFs.

The $PDFF_{ratio}$ also had high diagnostic performance at a cut-off value of ≤0.2 for malignancy: with 44 of 46 benign and 39 of 41 malignant fractures being correctly classified, two false-positive (osteoporotic) and two false-negative (multiple myeloma) findings, this resulted in a sensitivity of 96%, a specificity of 95% with a corresponding AUC of 97% (95% CI, 94-100%; $p < 0.001$), a PPV of 94%, an NPV of 96% and an accuracy of 95% in the differentiation of benign from malignant VCFs.

Further multivariate analysis revealed that PDFF remained as a significant imaging variable to independently differentiate between benign and malignant VCFs, yielding an odds ratio of 0.454 (95% CI, 0.263-0.783; $p = 0.005$).

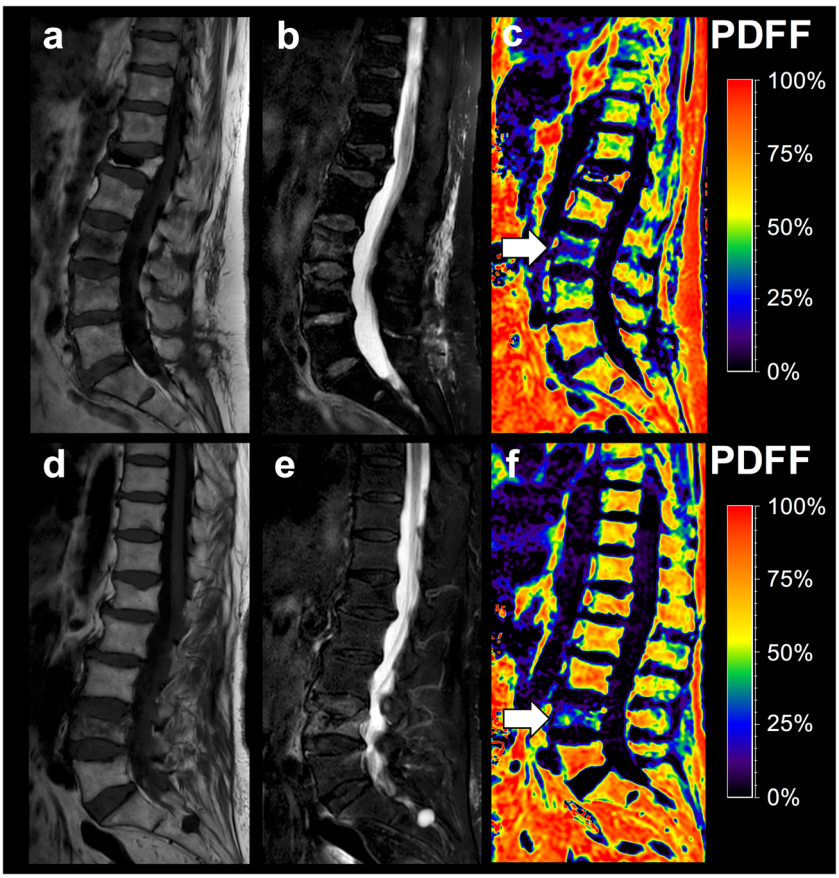

Fig. 1 Assessment of proton density fat fraction (PDFF) derived from six-echo modified Dixon (6E-mDixon) in acute osteoporotic vertebral compression fractures (VCFs). **a-c** Image set of a 65-year-old woman with an acute osteoporotic VCF of the L3 vertebral body. Sagittal T1-weighted (**a**) and T2-SPAIR-weighted (**b**) images and the corresponding PDFF map (**c**) with a coloured PDFF %-value scale demonstrating a mean PDFF of 18.1% within the fracture, indicating an acute osteoporotic VCF. **d-f** Image set of an 82-year-old woman with a pathologically confirmed acute osteoporotic VCF of the L4 vertebral body. Sagittal T1-weighted (**d**) and T2-SPAIR-weighted (**e**) images and the corresponding PDFF map (**f**) showing an intravertebral PDFF of 22.4%, which is suggestive of an acute benign VCF

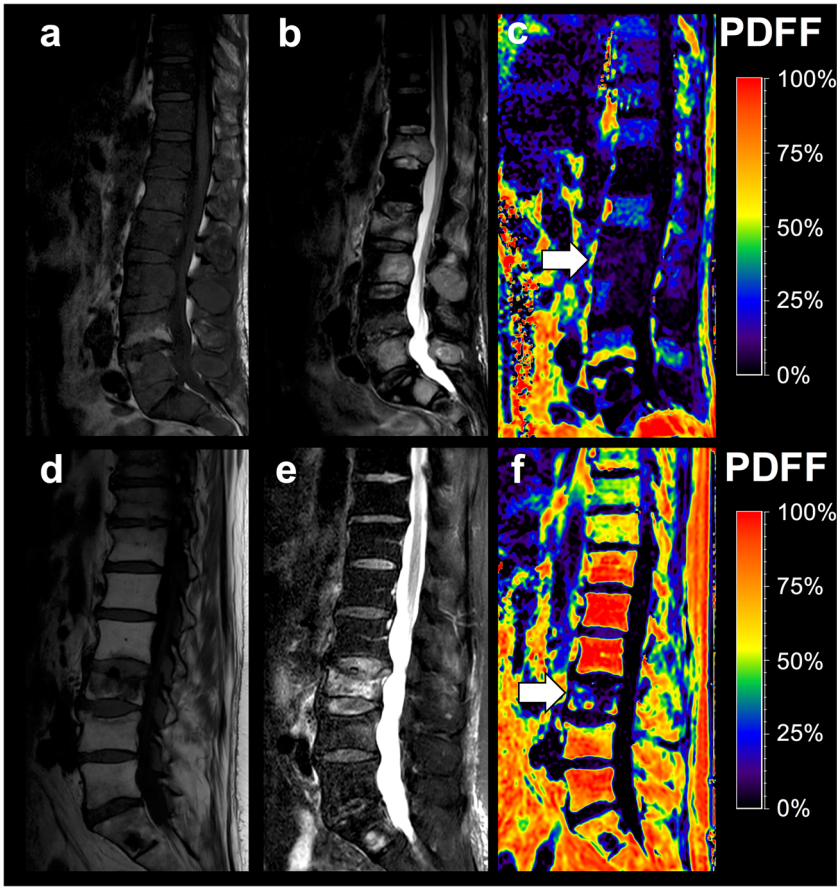

Fig. 2 Assessment of proton density fat fraction (PDFF) derived from six-echo modified Dixon (6E-mDixon) in malignant vertebral compression fractures (VCFs). **a-c** Image set of a 51-year-old man with osseous metastasis from non-small cell lung cancer and malignant VCF of the L2 vertebral body. Sagittal T1-weighted (**a**) and T2-SPAIR-weighted (**b**) images. The corresponding PDFF map with a coloured PDFF %-value scale (**c**) shows an intravertebral PDFF of 1.8%, which is suggestive of a malignant lesion. **d-f** Image set of a 63-year-old man with osseous metastasis from prostate cancer and biopsy proven malignant VCF of the L2 vertebral body. T1-weighted (**d**) and T2-SPAIR-weighted (**e**) images and the corresponding PDFF map (**f**) showing an intravertebral PDFF of 3.4%, indicating the fracture is malignant

Among the remaining significant imaging and clinical variables including $PDFF_{ratio}$, normal vertebrae PDFF, sex, prior chemotherapy and prior radiotherapy, only prior chemotherapy remained as a further statistically significant parameter to independently predict the nature of benign and malignant VCFs with an odds ratio of 0.05 (95% CI, 0.000-0.903; $p = 0.046$).

Discussion

This study evaluated the diagnostic performance of PDFF derived from 6E-mDixon to differentiate acute benign from malignant VCFs. The main study result is that the PDFF of acute benign VCFs is significantly higher than that of malignant VCFs, allowing differentiation of these two fracture types with

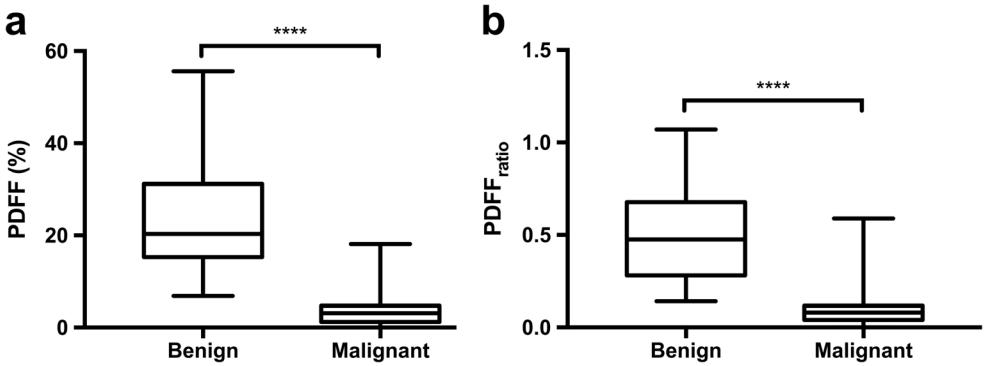

Fig. 3 Box-whisker plots of acute benign and malignant vertebral compression fractures (VCFs) demonstrating summary values of the absolute mean percentage proton density fat fraction (PDFF) (**a**) and the $PDFF_{ratio}$ (fracture PDFF/normal vertebrae PDFF) (**b**) as determined by six-echo modified Dixon (6E-mDixon). *Vertical solid lines* show minimum (*lower*) and maximum (*upper*) observations, respectively. *Boxes* represent the data between the 25th percentile and the 75th percentile. Median is shown as a *horizontal line* across each box. Malignant VCFs tend to show significantly lower PDFF values than acute benign VCFs (****$p < 0.0001$)

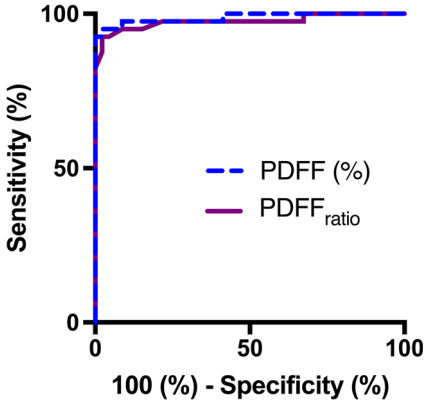

Fig. 4 Receiver operating characteristic (ROC) curves for the various six-echo modified Dixon (6E-mDixon) derived mean percentage proton density fat fraction (PDFF) values (**a**, *blue line*) and the $PDFF_{ratio}$ (fracture PDFF/normal vertebrae PDFF) (**b**, *purple line*) for the differentiation between acute benign and malignant compression fractures of the spine

high diagnostic accuracy. By using a PDFF cut-off value of ≤9% for malignancy, ROC curves yielded a sensitivity of 98% and a specificity of 95% with a corresponding AUC of 97% in the differentiation of benign from malignant VCFs. These results were accomplished with an excellent accuracy of 96%, a PPV of 94% and an NPV of 98% for differentiation of benign from malignant VCFs. $PDFF_{ratio}$ also allowed for a highly accurate differentiation between acute benign and malignant VCFs, albeit slightly weaker than the absolute fracture PDFF.

Quantitative water-fat MRI has previously been performed to differentiate focal benign from malignant skeletal lesions. Our current results are widely consistent with and extend those from prior reports regarding the fat content of benign and malignant lesions. Yoo et al. [20] found a PDFF cut-off value of 6.34% in order to distinguish benign from malignant bone marrow abnormalities of the spine. With regard to vertebral fractures that study was limited due to the inclusion of only a small number of benign fractures and total lack of assessment of malignant VCFs. Schmeel et al. [21] reported a sensitivity of 97.4% and a specificity of 91.3% in the differentiation between benign and malignant spine lesions using a PDFF cut-off value of ≤6.4% for malignancy. In that study, the same cut-off value was also highly specific in separating acute vertebral fractures from malignant lesions. However, malignant VCFs were also not included in that analysis. So far only one retrospective study has assessed the feasibility of PDFF for the differentiation between osteoporotic and malignant fractures by using a PDFF cut-off value of <5.26% [22]. With an AUC of 0.98, the diagnostic performance was on a similarly high level as in our observations. However, histopathological confirmation was available only in less than 5% of VCFs, and patient age varied significantly between the study groups. Since ageing is accompanied by a continual increase in the relative fat fraction of bone marrow [23], it is possible that the imbalance in age might introduce a bias in PDFF measurements, resulting in an overestimation of the differences between benign and malignant VCFs. Therefore, the question remains whether PDFF can help to indeed differentiate between benign and malignant VCFs.

Our study provides evidence for an excellent inter-reader reliability and a high diagnostic accuracy of PDFF in order to distinguish acute benign from malignant VCFs. Although bone biopsy is generally considered as the diagnostic gold standard, its invasiveness and the limitation to well accessible target lesions are reasons for a restrictive clinical use. Another shortcoming of biopsy is the inherent limitation to a very small specimen size, as a result of which focal bone marrow involvement may be missed. Our analysis shows that PDFF could independently differentiate the nature of VCFs on multivariate analysis, even after adjustment for the effects of prior chemotherapy. Owing to the high sensitivity and NPV of PDFF, this could eventually prevent patients from potentially harmful bone biopsy whilst allowing for further therapy planning.

Previous studies have successfully applied conventional in-phase/opposed-phase MRI to semi-quantitatively differentiate benign from malignant VCFs [7]. Reported sensitivities and specificities ranged up to 95% and 100%, respectively [24]. Recently, Geith et al. demonstrated that the signal loss in opposed-phase versus in-phase images was significantly lower in malignant than in osteoporotic VCFs, yielding an accuracy of 71.7% with a corresponding sensitivity of 50% and a specificity of 88.5% at a cut-off value of ≥-1.44 for malignancy [5]. However, several confounding factors are known to influence the ability of in-phase/opposed-phase MRI to quantify bone marrow fat content, including T1 bias and T2* effects. First, T1 relaxation times are widely divergent amongst water and fat compartments in bone marrow [25]. Second, the presence of trabecular bone in general shortens the T2* relaxation times, which are different for the water and fat components and can confound bone marrow fat quantification especially at high field strengths [26]. Moreover, most conventional chemical-shift-encoded MRI techniques assume that fat has as a single spectral peak, although multiple spectral peaks generally exist. This will lead to misidentification of fat signal as arising from water, leading to significant quantification errors [27]. Multi-echo mDixon water-fat MRI techniques such as 6E-mDixon can minimise the effects of T1-bias by using low flip angle excitation [28], incorporate a multipeak spectral model with several lipid components [29] and correct for the T2* signal decay in trabecular bone [13; 14]. Thus, previous studies have shown an excellent agreement between the PDFF derived from 6E-mDixon and fat-fraction estimations from *ex-vivo* trabecular bone phantoms [30] and semi-automatic histopathological fat quantification techniques [31]. Moreover, a recent meta-analysis reported on high linearity and precision of PDFF across different field strengths and imaging platforms [32].

We observed one false-positive diagnosis in a traumatically collapsed VCF of the lumbar spine. The reason for this finding is uncertain; however, previous research suggests that noise-related T1 bias and T2* effects may confound the determination of fat remnants in severely impacted bone [22]. We also observed a significant shortening of T2* within the tightly wedged vertebral body when compared to normal vertebrae, which, in combination with "true" marrow fat displacement, may have led to this false-positive observation. Two VCFs from multiple myeloma were rated falsely negative, whereas five remaining cases of multiple myeloma were correctly classified as malignant. Previous findings on multiple myeloma being a potential cause for false negative findings with respect to malignancy on both quantitative water-fat and conventional in-phase/opposed-phase MRI confirm our findings [21, 33]. In this respect, lymphoproliferative neoplasms may hold a special position within malignant bone lesions because they tend to preserve an amount of marrow fat among neoplastic cells at initial disease stages [34].

We acknowledge several limitations of this study. One limitation is the inclusion of different types of malignant primary tumours. This may have caused different PDFF values depending on the primary tumour but should not have changed overall findings. Another limitation is the small sample size, but the initial sample size considerations indicate that sufficient statistical power is provided. The fact that pathological correlation was available in 30 patients whilst the remaining patients, especially patients with benign fractures did not undergo biopsy may be regarded as a limitation of this study. However, ethical considerations usually prohibit a bioptic verification in all cases of apparently osteoporotic fractures. Lastly, apart from its diagnostic value, further research is needed to elucidate whether PDFF MRI could also prove useful for therapy management and follow-up of acute VCFs.

In conclusion, PDFF measurements derived from 6E-mDixon provide high diagnostic accuracy for the non-invasive differentiation between acute benign and malignant VCFs. High sensitivity and NPVs, fast imaging, and independence of contrast media make PDFF an ideal diagnostic approach for assessing VCFs.

Funding The authors state that this work has not received any funding.

Compliance with ethical standards

Guarantor The scientific guarantor of this publication is Priv.-Doz. Dr. med. Guido Matthias Kukuk at Bonn University Hospital.

Conflict of interest The authors of this manuscript declare no relationships with any companies, whose products or services may be related to the subject matter of the article.

Statistics and biometry No complex statistical methods were necessary for this paper.

Informed consent Written informed consent was obtained from all patients in this study.

Ethical approval Institutional Review Board approval was obtained.

Methodology
- prospective
- diagnostic or prognostic study
- performed at one institution

References

1. Chapman J, Smith JS, Kopjar B et al (2013) The AOSpine North America Geriatric Odontoid Fracture Mortality Study: a retrospective review of mortality outcomes for operative versus nonoperative treatment of 322 patients with long-term follow-up. Spine (Phila Pa 1976) 38:1098–1104
2. Hansen EJ, Simony A, Carreon L, Andersen MO (2016) Rate of unsuspected malignancy in patients with vertebral compression fracture undergoing percutaneous vertebroplasty. Spine (Phila Pa 1976) 41:549–552
3. Jung HS, Jee WH, McCauley TR, Ha KY, Choi KH (2003) Discrimination of metastatic from acute osteoporotic compression spinal fractures with MR imaging. Radiographics 23:179–187
4. Link TM, Guglielmi G, van Kuijk C, Adams JE (2005) Radiologic assessment of osteoporotic vertebral fractures: diagnostic and prognostic implications. Eur Radiol 15:1521–1532
5. Geith T, Schmidt G, Biffar A et al (2012) Comparison of qualitative and quantitative evaluation of diffusion-weighted MRI and chemical-shift imaging in the differentiation of benign and malignant vertebral body fractures. AJR Am J Roentgenol 199:1083–1092
6. Disler DG, McCauley TR, Ratner LM, Kesack CD, Cooper JA (1997) In-phase and out-of-phase MR imaging of bone marrow: prediction of neoplasia based on the detection of coexistent fat and water. AJR Am J Roentgenol 169:1439–1447
7. Zajick DC Jr, Morrison WB, Schweitzer ME, Parellada JA, Carrino JA (2005) Benign and malignant processes: normal values and differentiation with chemical shift MR imaging in vertebral marrow. Radiology 237:590–596
8. Erly WK, Oh ES, Outwater EK (2006) The utility of in-phase/opposed-phase imaging in differentiating malignancy from acute benign compression fractures of the spine. AJNR Am J Neuroradiol 27:1183–1188
9. Eito K, Waka S, Naoko N, Makoto A, Atsuko H (2004) Vertebral neoplastic compression fractures: assessment by dual-phase chemical shift imaging. J Magn Reson Imaging 20:1020–1024
10. Douis H, Davies AM, Jeys L, Sian P (2016) Chemical shift MRI can aid in the diagnosis of indeterminate skeletal lesions of the spine. Eur Radiol 26:932–940
11. Fischer MA, Nanz D, Shimakawa A et al (2013) Quantification of muscle fat in patients with low back pain: comparison of multi-echo MR imaging with single-voxel MR spectroscopy. Radiology 266: 555–563
12. Ruschke S, Pokorney A, Baum T et al (2017) Measurement of vertebral bone marrow proton density fat fraction in children using quantitative water-fat MRI. MAGMA 30:449–460
13. Gee CS, Nguyen JT, Marquez CJ et al (2015) Validation of bone marrow fat quantification in the presence of trabecular bone using MRI. J Magn Reson Imaging 42:539–544
14. Karampinos DC, Melkus G, Baum T, Bauer JS, Rummeny EJ, Krug R (2014) Bone marrow fat quantification in the presence of trabecular bone: initial comparison between water-fat imaging and single-voxel MRS. Magn Reson Med 71:1158–1165

15. Latifoltojar A, Hall-Craggs M, Bainbridge A et al (2017) Whole-body MRI quantitative biomarkers are associated significantly with treatment response in patients with newly diagnosed symptomatic multiple myeloma following bortezomib induction. Eur Radiol 27: 5325–5336
16. Baker LL, Goodman SB, Perkash I, Lane B, Enzmann DR (1990) Benign versus pathologic compression fractures of vertebral bodies: assessment with conventional spin-echo, chemical-shift, and STIR MR imaging. Radiology 174:495–502
17. Minne HW, Leidig G, Wuster C et al (1988) A newly developed spine deformity index (SDI) to quantitate vertebral crush fractures in patients with osteoporosis. Bone Miner 3:335–349
18. Mauch JT, Carr CM, Cloft H, Diehn FE (2018) Review of the imaging features of benign osteoporotic and malignant vertebral compression fractures. AJNR Am J Neuroradiol. https://doi.org/10.3174/ajnr.A5528
19. Faul F, Erdfelder E, Buchner A, Lang AG (2009) Statistical power analyses using G*Power 3.1: tests for correlation and regression analyses. Behav Res Methods 41:1149–1160
20. Yoo HJ, Hong SH, Kim DH et al (2017) Measurement of fat content in vertebral marrow using a modified dixon sequence to differentiate benign from malignant processes. J Magn Reson Imaging 45: 1534–1544
21. Schmeel FC, Luetkens JA, Wagenhauser PJ et al (2018) Proton density fat fraction (PDFF) MRI for differentiation of benign and malignant vertebral lesions. Eur Radiol. https://doi.org/10.1007/s00330-017-5241-x
22. Kim DH, Yoo HJ, Hong SH, Choi JY, Chae HD, Chung BM (2017) Differentiation of acute osteoporotic and malignant vertebral fractures by quantification of fat fraction with a Dixon MRI sequence. AJR Am J Roentgenol 209:1331–1339
23. Kugel H, Jung C, Schulte O, Heindel W (2001) Age- and sex-specific differences in the 1H-spectrum of vertebral bone marrow. J Magn Reson Imaging 13:263–268
24. Ragab Y, Emad Y, Gheita T et al (2009) Differentiation of osteoporotic and neoplastic vertebral fractures by chemical shift {in-phase and out-of phase} MR imaging. Eur J Radiol 72:125–133
25. Baum T, Yap SP, Dieckmeyer M et al (2015) Assessment of whole spine vertebral bone marrow fat using chemical shift-encoding based water-fat MRI. J Magn Reson Imaging 42:1018–1023
26. Karampinos DC, Ruschke S, Dieckmeyer M et al (2015) Modeling of T2* decay in vertebral bone marrow fat quantification. NMR Biomed 28:1535–1542
27. Reeder SB, Robson PM, Yu H et al (2009) Quantification of hepatic steatosis with MRI: the effects of accurate fat spectral modeling. J Magn Reson Imaging 29:1332–1339
28. Karampinos DC, Yu H, Shimakawa A, Link TM, Majumdar S (2011) T(1)-corrected fat quantification using chemical shift-based water/fat separation: application to skeletal muscle. Magn Reson Med 66:1312–1326
29. Hines CD, Yu H, Shimakawa A, McKenzie CA, Brittain JH, Reeder SB (2009) T1 independent, T2* corrected MRI with accurate spectral modeling for quantification of fat: validation in a fat-water-SPIO phantom. J Magn Reson Imaging 30:1215–1222
30. Bray TJP, Bainbridge A, Punwani S, Ioannou Y, Hall-Craggs MA (2017) Simultaneous quantification of bone edema/adiposity and structure in inflamed bone using chemical shift-encoded mri in spondyloarthritis. Magn Reson Med 79:1031–1042
31. Kukuk GM, Hittatiya K, Sprinkart AM et al (2015) Comparison between modified Dixon MRI techniques, MR spectroscopic relaxometry, and different histologic quantification methods in the assessment of hepatic steatosis. Eur Radiol 25:2869–2879
32. Yokoo T, Serai SD, Pirasteh A et al (2017) Linearity, bias, and precision of hepatic proton density fat fraction measurements by using MR imaging: a meta-analysis. Radiology 286:486–498
33. Zampa V, Cosottini M, Michelassi C, Ortori S, Bruschini L, Bartolozzi C (2002) Value of opposed-phase gradient-echo technique in distinguishing between benign and malignant vertebral lesions. Eur Radiol 12:1811–1818
34. Stabler A, Baur A, Bartl R, Munker R, Lamerz R, Reiser MF (1996) Contrast enhancement and quantitative signal analysis in MR imaging of multiple myeloma: assessment of focal and diffuse growth patterns in marrow correlated with biopsies and survival rates. AJR Am J Roentgenol 167:1029–1036